Available online at www.sciencedirect.com

SCIENCE DIRECT®

Tectonophysics 391 (2004) 259–282

TECTONOPHYSICS

www.elsevier.com/locate/tecto

From transpression to transtension: changes in morphology and structure around a bend on the North Anatolian Fault in the Marmara region

Aral I. Okay[a,*], Okan Tüysüz[a], Şinasi Kaya[b]

[a]*Eurasia Institute of Earth Sciences, Istanbul Technical University, Ayazağa 34469, İstanbul, Turkey*

[b]*Department of Geodesy and Photogrammetry, Faculty of Civil Engineering, Istanbul Technical University, Ayazağa 34469, İstanbul, Turkey*

Accepted 3 June 2004

Available online 11 September 2004

Abstract

The east–west-trending North Anatolian Fault makes a 17° bend in the western Marmara region from a mildly transpressional segment to a strongly transtensional one. We have studied the changes in the morphology and structure around this fault bend using digital elevation models, field structural geology, and multi-channel seismic reflection profiles. The transpression is reflected in the morphology as the Ganos Mountain, a major zone of uplift, 10 km wide and 35 km long, elongated parallel to the transpressional Ganos Fault segment west of this bend. Flat-lying Eocene turbidites of the Thrace Basin are folded upwards against this Ganos Fault, forming a monocline with the Ganos Mountain at its steep southern limb and the flat-lying hinterland farther north at the flat limb. The sharp northern margin of the Ganos Mountain coincides closely with the monoclinal axis. The strike of the bedding, and the minor and regional fold axes in the Eocene turbidites in Ganos Mountain are parallel to the trace of the Ganos Fault indicating that these structures, as well as the morphology, have formed by shortening perpendicular to the North Anatolian Fault. The monoclinal structure of Ganos Mountain implies that the North Anatolian Fault dips under this mountain at 50°, and this ramp terminates at a decollement at a calculated depth of ~8 km. East of this fault bend, the northward dip of the North Anatoxlian Fault is maintained but it has a normal dip-slip component. This has led to the formation of an asymmetric half-graben, the Tekirdağ Basin in the western Sea of Marmara, containing a thickness of up to 2.5 km of Pliocene to Recent syn-transform sediments. As the Ganos uplift is translated eastwards from the transpressional to the transtensional zone, it undergoes subsidence by southward tilting. However, a morphological relic of the Ganos uplift is maintained as the steep northern submarine slope of the Tekirdağ Basin. The minimum of 3.5 km of fault-normal shortening in the Ganos Mountain, and the minimum of 40 km eastward translation of the Ganos uplift indicate that the present fault geometry has existed for at least the last 2 million years.

Keywords: Transpression; Transtension; North Anatolian Fault; Marmara; Morphology; Turkey

* Corresponding author. Tel.: +90 212 285 6208; fax: +90 212 285 6210.

E-mail address: okay@itu.edu.tr (A.I. Okay).

0040-1951/$ - see front matter © 2004 Elsevier B.V. All rights reserved.

doi:10.1016/j.tecto.2004.07.016

1. Introduction

We have investigated a major fault bend along the North Anatolian Fault in the western Marmara region using geodetic data, digital elevation models, field structural studies, and seismic reflection profiles. The aim was to understand the mechanics and kinematics of changes in the morphology and in the structure associated with a transition from transpression to transtension. In particular we explored the fate of the transpressive structures and morphology as they are transported to a transtensional environment. Geodetic measurements indicate the present strain field, the morphology reveals recent vertical movements and erosion, and the structures in the rocks give the finite strain over at least the past several million years. Integration of data from these three sources enables an understanding of the evolution of structures over time.

The North Anatolian fault is a major dextral transform fault, which accommodates the westward motion of the Anatolian Plate (Fig. 1). It extends for ~1600 km from the Karlıova triple junction in the east to the North Aegean Trough in the Aegean Sea in the west (e.g., Şengör, 1979; Barka, 1992; Westaway, 1994; Hubert-Ferrari et al., 2002). Until recently, it was generally accepted that the North Anatolian fault became active around the start of the Pliocene (e.g., Barka, 1992). Recent regional models (Westaway, 2003, 2004) suggest instead that the North Anatolian fault first became active towards the end of the Miocene, but its present geometry developed in the Pliocene.

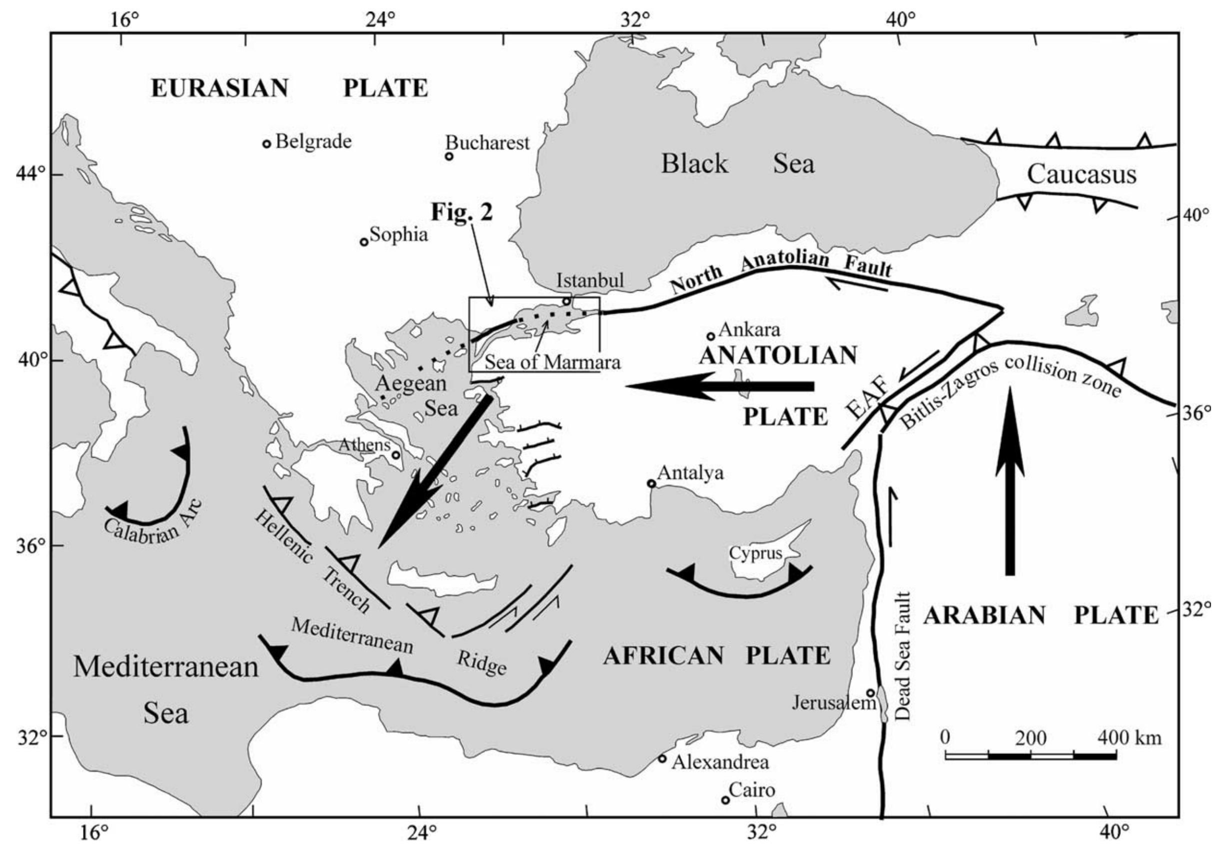

Fig. 1. Active tectonic map of the Eastern Mediterranean showing the geological setting of the Sea of Marmara. Lines with filled triangles show active subduction zones, lines with open triangles are active thrust faults at continental collision zones, and lines with thick marks are normal faults. The large solid arrows indicate approximate senses of motion of the lithospheric plates relative to Eurasia. EAF, East Anatolian Fault.

Although primarily a transform fault, along its entire length the North Anatolian Fault zone is associated with uplifts and depressions related to segmentation and bending. The most prominent active depressions are the three basins, over 1000 m deep, which are forming along its main strand in the Sea of Marmara (Wong et al., 1995; Okay et al., 2000; Le Pichon et al., 2001; Armijo et al., 2002; Fig. 2). In this paper we are concerned with the western depression, the Tekirdağ Basin, and the adjoining Ganos Mountain farther west. These are forming around the Ganos bend between the Central Marmara and Ganos segments of the North Anatolian Fault (Fig. 2). This bend is thought to mark the eastern termination of fault rupture in the M_S 7.4 Saros–Marmara earthquake of 9 August 1912 (Ambraseys and Finkel, 1987).

2. Fault geometry, obliquity and amounts of fault normal shortening or extension

Within any strike-slip fault zone, the angle of obliquity, α, between the strike of any fault plane and the displacement vector provides a measure of transpression or transtension (cf. Westaway, 1995). Transform fault segments, which strike parallel to the regional displacement vector, require no distributed deformation in their surroundings. Faults with other orientations require such deformation, which is characterised by either fault-normal extension or shortening, either on their own or in combination with components of distributed vertical simple shear (cf. Westaway, 1995). Westaway (1995) obtained analytic solutions relating these components of deformation to observable quantities such as the obliquity of strike and kinematic indicators (such as orientations of fold axes and small-scale faulting, and amounts of finite strain and vertical-axis rotation). However, these solutions have not been used in this study, because their derivation assumed that the principal strike-slip faults are vertical whereas it seems clear from the available evidence (see below) that in the present study region these faults dip at angles that are well away from the vertical.

Both the strike of the fault plane and the displacement vector are known in the Marmara region. The trace of the Ganos Fault onland is tightly constrained from geology, topography, air photos and satellite imagery (Allen, 1975; Ambraseys and Finkel, 1987; Okay et al., 1999; Rockwell et al., 2001; Fig. 3a). The Ganos Fault thus forms a 45-km-long linear fault zone consisting of several subparallel segments, which are offset by less than 1 km (Fig. 3). The eastern segment trends N70°±1°E. This observed linearity of the Ganos Fault trace indicates that it provides a close approximation to the strike of the fault plane. The geometry of the North Anatolian Fault under the Marmara Sea is now also well known from detailed multi-beam bathymetry, multi-channel seismic and deep-towed seismic data (Okay et al., 1999; Rangin et al., 2001; İmren et al., 2001; Le Pichon et al., 2001; Armijo et al., 2002; Demirbağ et al., 2003; Fig. 3a). The Ganos Fault enters the Sea of Marmara at the village of Gaziköy and continues offshore maintaining its N70°E trend (Seeber et al., 2004). Its continuation is obscured by a large submarine slide, caused by the collapse of the shelf edge that is composed of unlithified Miocene sands (Gazioğlu et al., 2002; Yaltırak, 2002). However, in most studies the North Anatolian Fault is shown as following the front of the submarine slide as a transpressive segment (Okay et al., 1999; Le Pichon et al., 2001; Armijo et al., 2002, Demirbağ et al., 2003; Seeber et al., 2004). Nonetheless, interpretation of seismic reflection section 2 (see below) indicates that this fault cuts this submarine slide. Continuous creep or episodic submarine sliding has probably obscured its trace within this submarine slide. The modified fault trace constructed from seismic reflection profiles and bathymetry shows a smoother fault bend over a distance of 10 km. The average strike of the Central Marmara Fault east of this bend is N87°±2°E (Le Pichon et al., 2001; Armijo et al., 2002), which gives a fault bend angle of 17±3°.

The relative displacement vectors in the Marmara region are known through a dense network of GPS stations (Straub et al., 1997; Meade et al., 2002). The measured slip vectors in the Anatolian Plate with respect to stable Eurasia exhibit a general anticlockwise rotation, and an increase in total displacement towards the west caused by the westward-increasing pull of the Hellenic subduction system (McClusky et al., 2000; Fig. 1). The GPS vectors in the three stations south of the Ganos Fault range in azimuth between 73° and 75° (72.8° on Marmara Island, MISL; 75.0° at Karabiğa, KABI; and 72.9° at

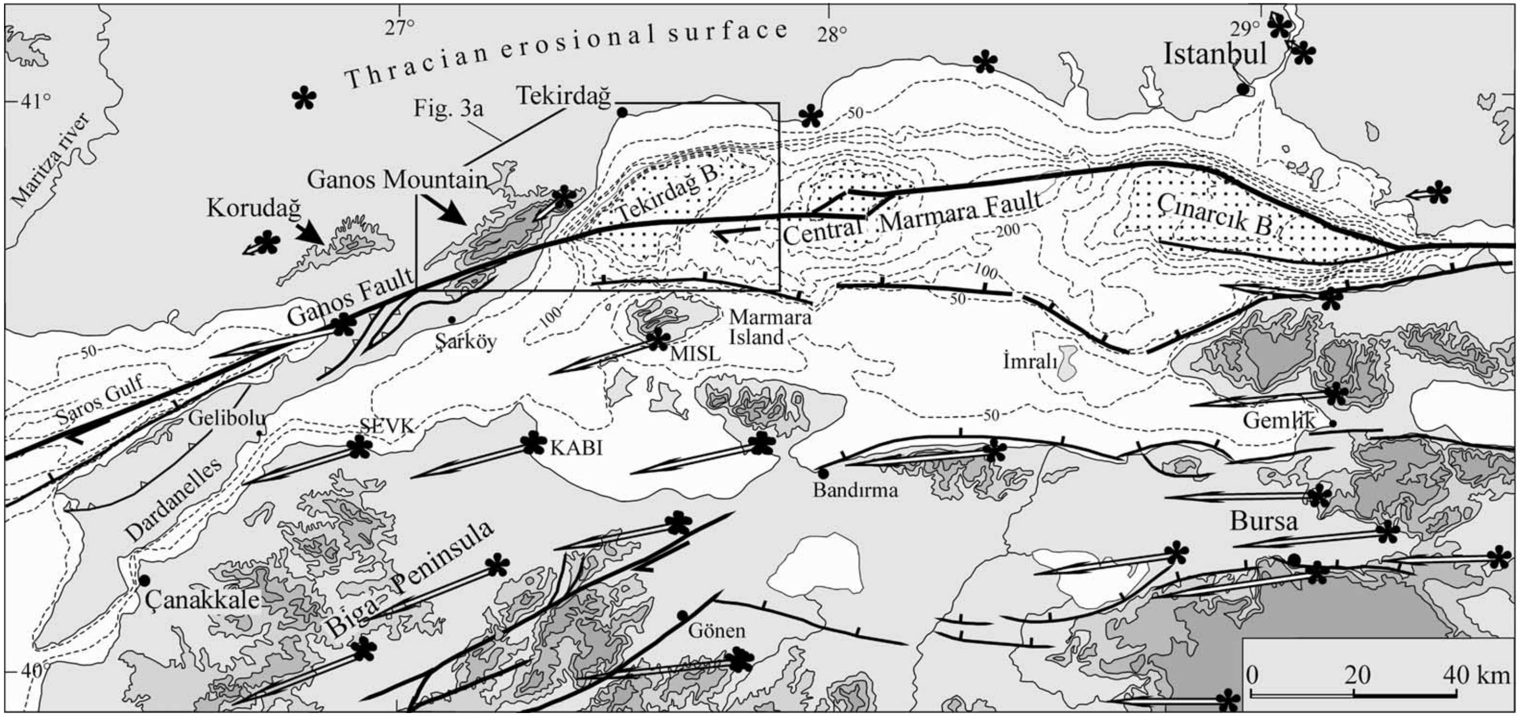

Fig. 2. Active faults in the Marmara region. For the location, see Fig. 1. The map is compiled from Şaroğlu et al. (1992), Okay et al. (1999, 2000), and Le Pichon et al. (2001). Faults shown cut Miocene or younger sediments. The bathymetric contours in the Marmara Sea are drawn at 50, 100, then at every 200 m. The topographic contours are at 300, 450 and 600 m. The stars and arrows indicate Global Positioning System (GPS) station localities and displacement vectors, respectively, with respect to stable Eurasia (McClusky et al., 2000; Meade et al., 2002).

Şevketiye, SEVK; using the data in Meade et al., 2002) (Fig. 2). A best fit polar rotation taking into account all the GPS stations in the Marmara region indicates a displacement vector towards 73° near the Ganos bend (Straub, 1996). The angle of obliquity, α, is thus $14 \pm 3°$ in the transtensive sense on the western Central Marmara Fault, and $3 \pm 1°$ in the transpressive sense on the eastern Ganos Fault.

The relative velocity between Anatolia and Eurasia in the western Marmara region is 22 ± 3 mm/yr (e.g., Kahle et al., 2000; McClusky et al., 2000; Meade et al., 2002). Historical seismicity (Ambraseys, 2002) and GPS data (Fig. 2) show that more than 90% of this strain is accumulating on the Ganos and Central Marmara faults. Taking an average velocity V of 20 mm/yr, the Ganos Fault accommodates fault-normal convergence at a rate of 1.1 ± 0.4 mm/yr, whereas the western end of the Central Marmara Fault accommodates fault-normal extension at 4.8 ± 1.0 mm/yr (both calculated as $V \sin \alpha$).

3. Transpression: Ganos Mountain, a ramp monocline

3.1. Morphology

Ganos Mountain is a region of anomalous uplift at the eastern end of the Ganos Fault (Fig. 3). It trends N70°E parallel to the Ganos Fault for ~35 km with a relatively uniform width of 8 to 11 km (Figs. 2 and 3). The steep northern submarine slope of the Tekirdağ Basin forms an integral part of the Ganos Mountain. The maximum relief is ~2000 m, from the base of the Tekirdağ depression at −1120 m to the summit at 924 m. Ganos Mountain is dissected by two transverse streams draining to the west, whose development is probably related to the progressive westward growth of this mountain (Keller et al., 1999). Towards the southwest, Ganos Mountain dies out sharply, giving way to the Saros depression of the Aegean Sea, whereas towards the northeast it projects into the steep northern submarine slope of the Tekirdağ Basin (Figs. 2 and 3). The southern margin of Ganos Mountain, defined by the Ganos Fault, is very abrupt and is characterized by very steep slopes of up to 50° (Fig. 3b). In the north, this mountain is bordered by the Thracian plain, a large, flat-lying erosion surface at ~120 m above sea-level, which probably formed during the Late Pliocene–Early Quaternary (Okay and Okay, 2002; Fig. 2). The abrupt transition from the Thracian plain to Ganos Mountain is well marked on the slope map and trends subparallel to the trace of the Ganos Fault (Fig. 3b). The parallel disposition of the northern and southern margins of the mountain with the Ganos Fault indicates that the Ganos uplift is controlled by the North Anatolian Fault, as previously deduced (e.g., Şengör, 1979).

Ganos Mountain forms essentially a single range made up of similar lithology, is relatively small, and has a uniform orientation. These geomorphic features, coupled with the high rate of deformation in the region, indicate that the morphology of this mountain can be used to chart recent vertical crustal motions. Furthermore, because this mountain lies at the coast, changes in uplift and subsidence can be quantified relative to sea level. Fig. 4 shows cross sections of Ganos Mountain parallel and perpendicular to the fault. The parallel cross section shows an increase in uplift towards the east, reaching a maximum value at ~2 km west of the coastline, and then rapid subsidence farther east. This is also seen in two cross sections perpendicular to the Ganos Fault, which are 11 km apart (Fig. 4a). Between these cross sections the structure maintains or even accentuates its relief towards the east but has subsided by ~1100 m, with the northern submarine slope of the Tekirdağ Basin forming the direct submarine continuation of the southern flank of Ganos Mountain. This eastward subsidence is also apparent in the geology, where the formation boundaries and average bedding strike out into the Marmara Sea (cf. Fig. 6).

The subsidence of Ganos Mountain is not uniform but increases towards the Ganos Fault indicating that it is largely achieved by southward tilting. This can be deduced by comparing the two subparallel cross sections in Fig. 4a. These show that the surface trace of the Ganos Fault has subsided by 1100 m between profiles A and B, whereas the surface trace of the upper stratigraphic boundary of the Gaziköy Formation has subsided by only 500 m. Furthermore, en bloc subsidence would have created a basin north of Ganos Mountain, which is not observed. Therefore most of the subsidence occurs by tilting with the tilt axis ~9–10 km north of the Ganos Fault (Fig. 4a).

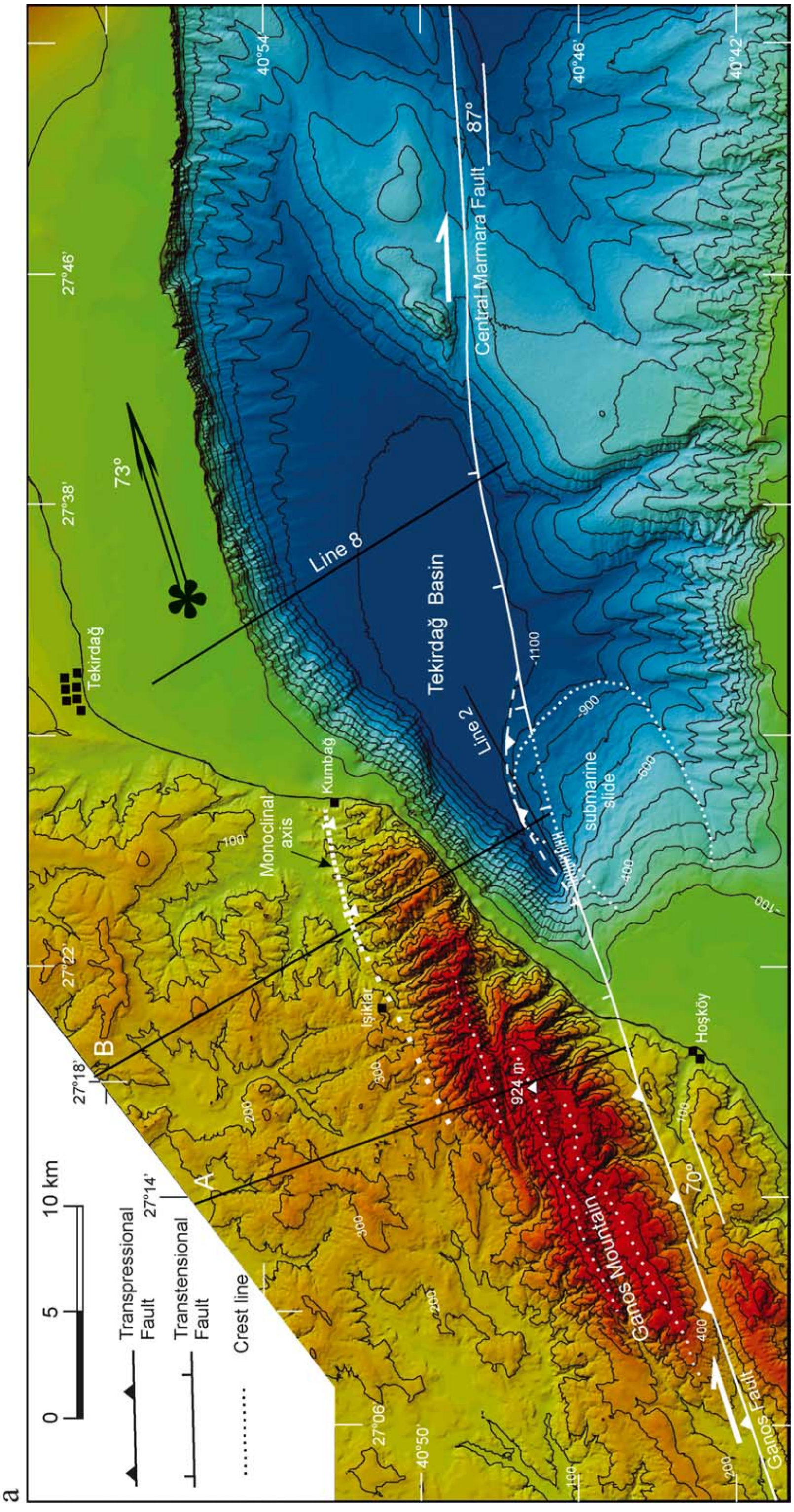
a
0
5
10 km
Transpressional Fault
Transtensional Fault
Crest line
Tekirdağ
Line 8
73°
Tekirdağ Basin
Central Marmara Fault
87°
Line 2
submarine slide
Kumbağ
Monoclinal axis
Işıklar
924 m
Hoşköy
Ganos Mountain
Ganos Fault
70°
A
B
27°06'
27°14'
27°18'
27°22'
27°38'
27°46'
40°50'
40°54'
40°46'
40°42'

b

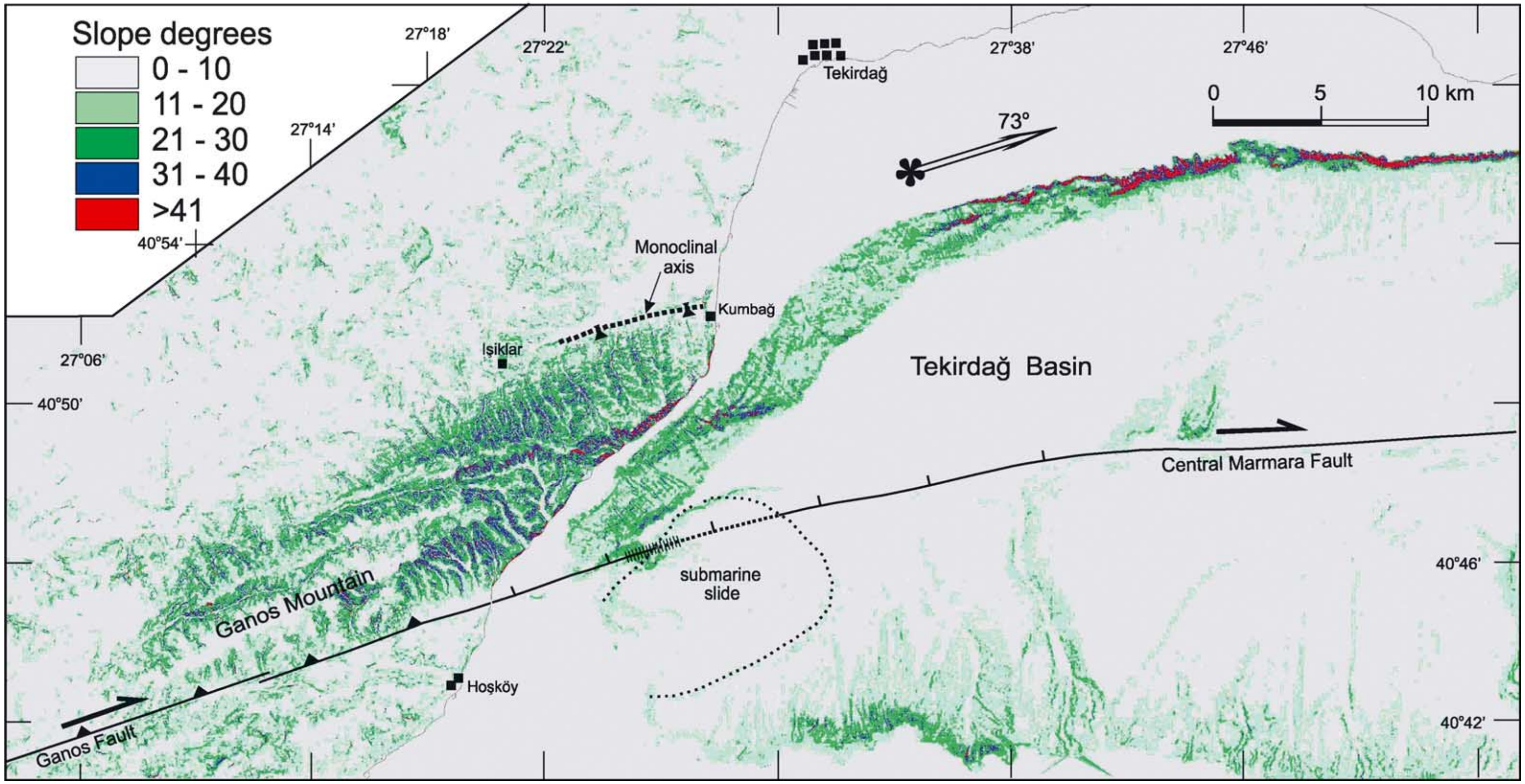

Fig. 3. (a) Digital elevation model of the Ganos Mountain and the adjoining Tekirdağ Basin. (b) Slope map of the Ganos Mountain and the adjoining Tekirdağ Basin. For both parts, topographic data were generated by digitising contour lines at every 20 m from 25 000 scale topographic maps. The shelf bathymetry is digitised from the bathymetric charts of SHOD (1983, 1988), whereas the bathymetry deeper than 100 m is produced from multibeam bathymetric data obtained by the research vessel Le Suroit (Rangin et al., 2001). All these data were combined and gridded using ER Mapper programme (v. 6.2) with all minimum curvature method. Each cell of the grid represents 20×20 m ground resolution. The data were sufficiently dense for such a small grid area except in the shelf, where the bathymetric measurements are relatively scarce. The hatched segment on the North Anatolian Fault marks the transition from transpression in the west to transtension in the east with a N73°E displacement vector.

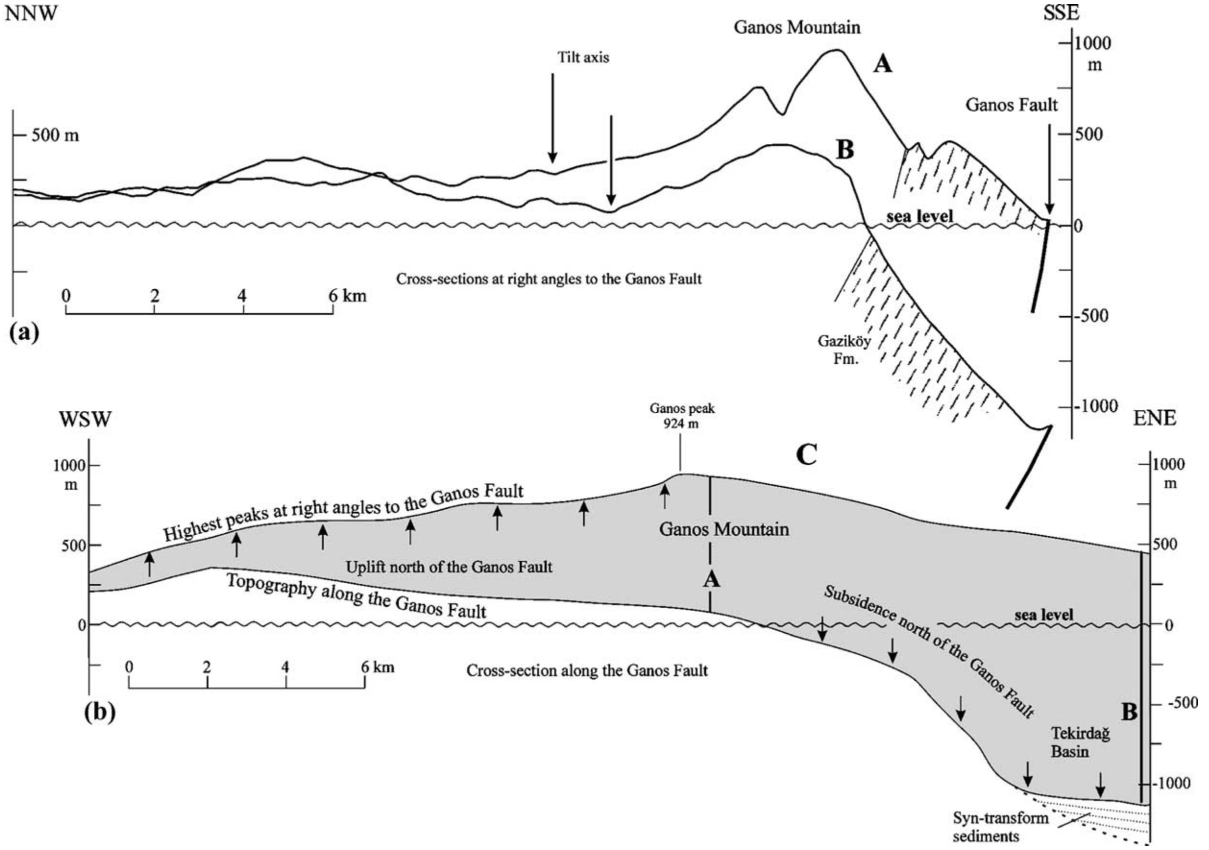

Fig. 4. (a) Cross sections from the Ganos Mountain and the adjoining Tekirdağ Basin projected perpendicular to the North Anatolian Fault. Profile B is 11 km ENE of profile A. For locations see Fig. 3. Note that both profiles A and B are similar, but B has subsided by more than 1000 m relative to A. (b) Projection of the Ganos Mountain on a vertical Ganos fault plane. The lower curve shows the topography along the Ganos Fault, and the upper curve the projection of the crest line of Ganos Mountain.

Southward tilting by ~7° is thus evident between profiles A and B, calculated as $\tan^{-1}$ (1.1 km/9 km). Distributed normal faulting at high angles to the Ganos Fault, with the fault planes consistently dipping to the northeast (see below), also contributes to the subsidence of Ganos Mountain.

Microbathymetry and shallow stratigraphy have been obtained from the region where the Ganos Fault juts out to the Marmara Sea (Polonia et al., 2002). Based on these data Seeber et al. (2004) also argue for subsidence and southward tilting of the north side of the Ganos Fault, the subsidence rate being estimated as 4–6 mm/yr. With this rather high rate, the subsidence between profiles A and B in Fig. 4 can be achieved in 183–275 ka, whereas the 11 km of strike slip displacement would take 550 ka at a rate of 20 mm/yr. Further studies are needed to solve the discrepancy between these two calculations. However, both of these calculations indicate that the subsidence of the Ganos Mountain has been continuing at least since several hundred thousand years ago.

Subsidence by southward tilting also explains an apparent anomaly. Although Ganos Mountain is subsiding in the east, it is still characterized by very steep slopes facing the Sea of Marmara. This produces a shoulder-type margin, with the drainage divide close to the top of the escarpment (Fig. 3). These types of margins are usually explained by uplift at the foot of the escarpment. However, in this case rotational normal faulting leads not only to subsidence but also to an increase in slope angles due to the southward tilting of the mountain face (Fig. 4a).

Some details in this region remain unexplained. Notably, extension starts several kilometres west of the Ganos bend, where the fault strike and slip vectors predict mild transpression. Furthermore, the strike of the fault trace does not change at the boundary between the regions of observed transpression and transtension.

3.2. Stratigraphy

Stratigraphically, Ganos Mountain forms an uplifted part of the hydrocarbon-bearing Mid-Eocene to Oligocene sequence of the Thrace Basin (Kopp et al., 1969; Turgut et al., 1991; Görür and Okay, 1996). This consists mainly of siliciclastic turbidites and is more than 9 km thick in its central part. These sedimentary rocks are weakly deformed except along the active North Anatolian fault and the inactive Terzili fault of Miocene age. Ganos Mountain exposes these Eocene–Oligocene siliciclastic rocks, which are divided into four formations (Figs. 5 and 6). The oldest, the Gaziköy Formation, consists mainly of Eocene shale and siltstone with rare sandstone and andesitic tuff and basaltic lava interbeds, and represents distal turbidites (Aksoy, 1987). Its base is not exposed, but it has a minimum measured thickness of 855 m and gradually passes up to the sandstone–shale intercalation of the Keşan Formation. The Keşan Formation has a thickness of over 3 km at Ganos Mountain and consists of Upper Eocene proximal turbidites. It is overlain conformably by shales of the Mezardere formation, 750 m thick, representing prodelta mudstones. These shales are overlain by the thickly bedded Oligocene sandstones of the Osmancık Formation.

The stratigraphy south of the Ganos Fault is different. In this region, which is morphologically not part of the Ganos Mountain, a sandy Miocene sequence, more than 1 km thick, unconformably overlies turbiditic Eocene–Oligocene siliciclastics exposed in the cores of faulted anticlines (Fig. 6; Okay et al., 1999; Sakınç et al., 1999; Yaltırak and Alpar, 2002). This difference is caused by the vertical movements along the North Anatolian Fault, which led to the erosion of the Miocene sequence north of the fault, as well as by the right-lateral offset on the North Anatolian Fault, which now juxtaposes regions that were previously separated by distances of tens of kilometres.

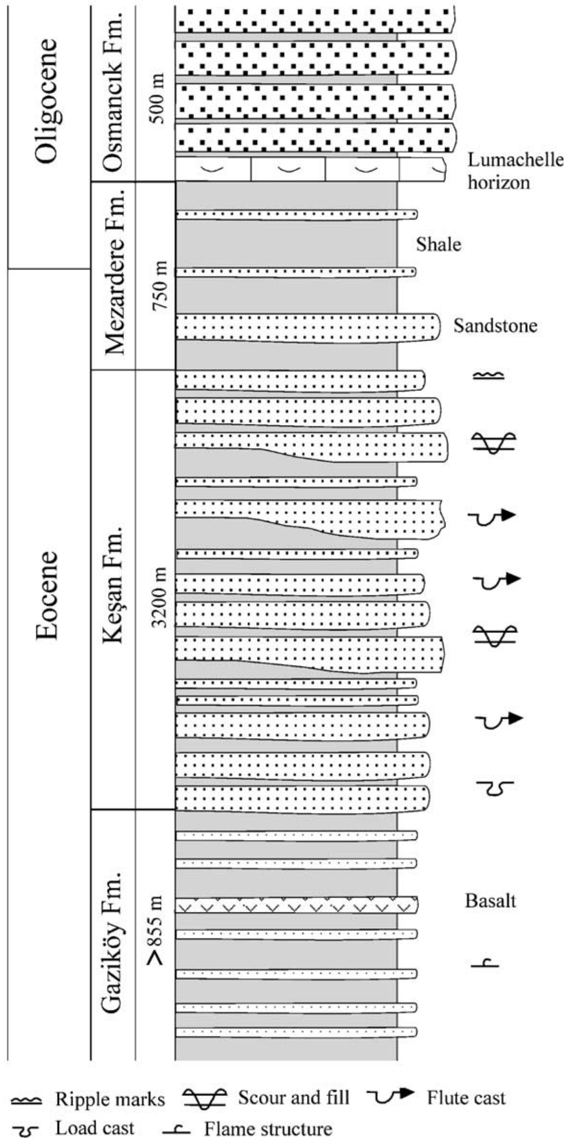

Fig. 5. Stratigraphy of Ganos Mountain (modified from Kopp et al., 1969; Aksoy, 1987; Turgut et al., 1991).

3.3. Structure

The structures south and north of the Ganos Fault are also different. South of the Ganos Fault the Miocene sequence is deformed by minor thrusts striking oblique to the Ganos Fault, and by many small and gentle anticlines and synclines with fold axes oblique to subparallel to the Ganos Fault

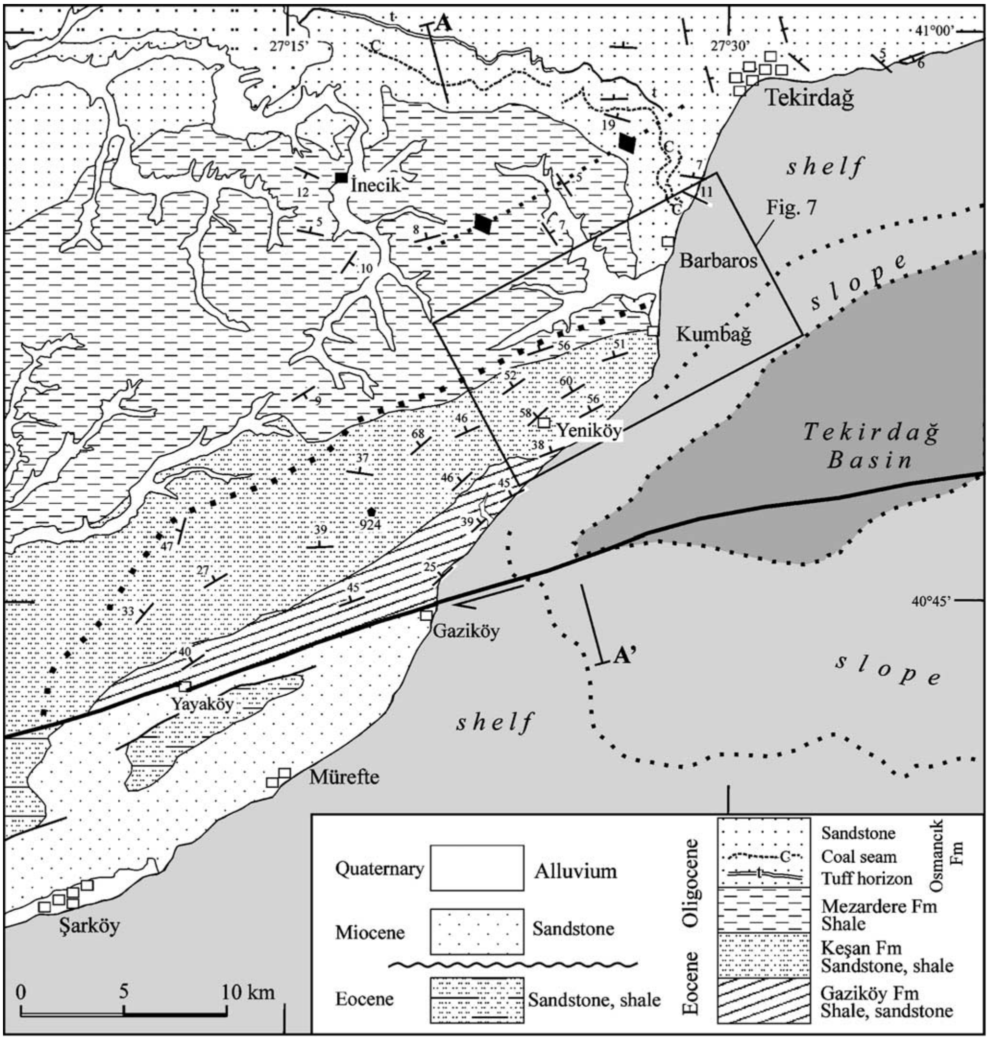

Fig. 6. Geological map of Ganos Mountain and the surrounding region. For location see Fig. 2 (compiled from Lebküchner, 1974; Şentürk et al., 1998; A. Okay unpublished data).

(Yaltırak, 1995; Tüysüz et al., 1998; Okay et al., 1999). In contrast, the structure north of the Ganos Fault is characterized by a crustal scale monocline, which provides significant information on the deep-seated geometry of the North Anatolian Fault. Ganos Mountain forms the steep southern limb of this monocline and the low-lying hinterland farther north its flat northern limb (Fig. 6). The zone of steep dips lies largely within the turbidites of the Gaziköy and Keşan formations, whereas the flat part is in the shales and sandstones of the Mezardere and Osmancık formations. The hinge trends parallel to the Ganos Fault and coincides closely with the northern margin of Ganos Mountain (Fig. 3b). The oldest rocks exposed are adjacent to the Ganos Fault, and the sequence youngs north–northwestward, away from this fault. The strikes of bedding and of the formation boundaries are subparallel to the Ganos Fault within a 10-km-wide zone north of the fault, although farther north the structures are highly oblique (Fig. 6). This is the case for the boundary between the Osmancık and Mezardere formations west of Barbaros, and for the coal seams in the Osmancık Formation, which define a large and gently east–northeast plunging anticline

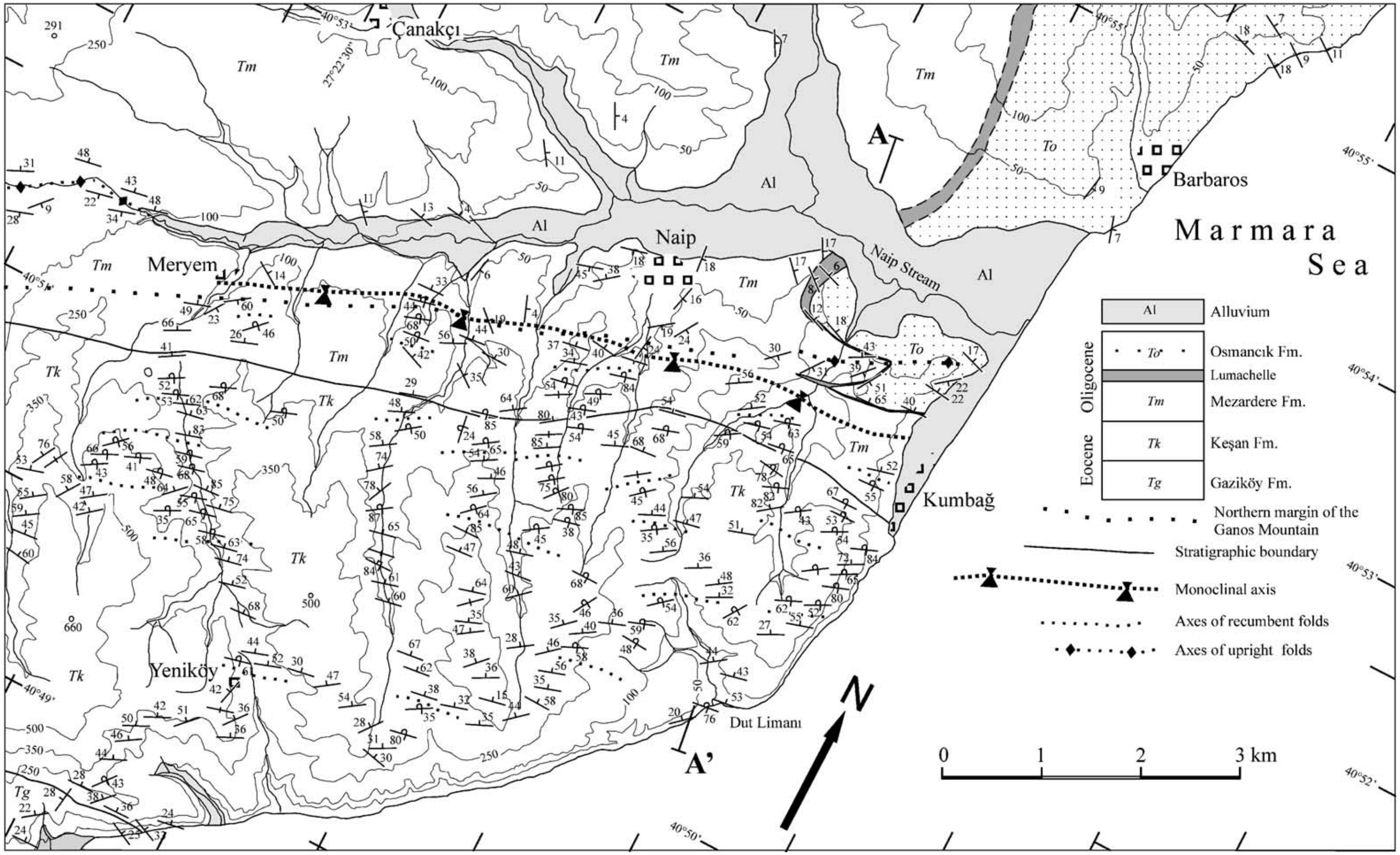

Fig. 7. Geological map of the Kumbağ region, eastern Ganos Mountain. For location see Fig. 6.

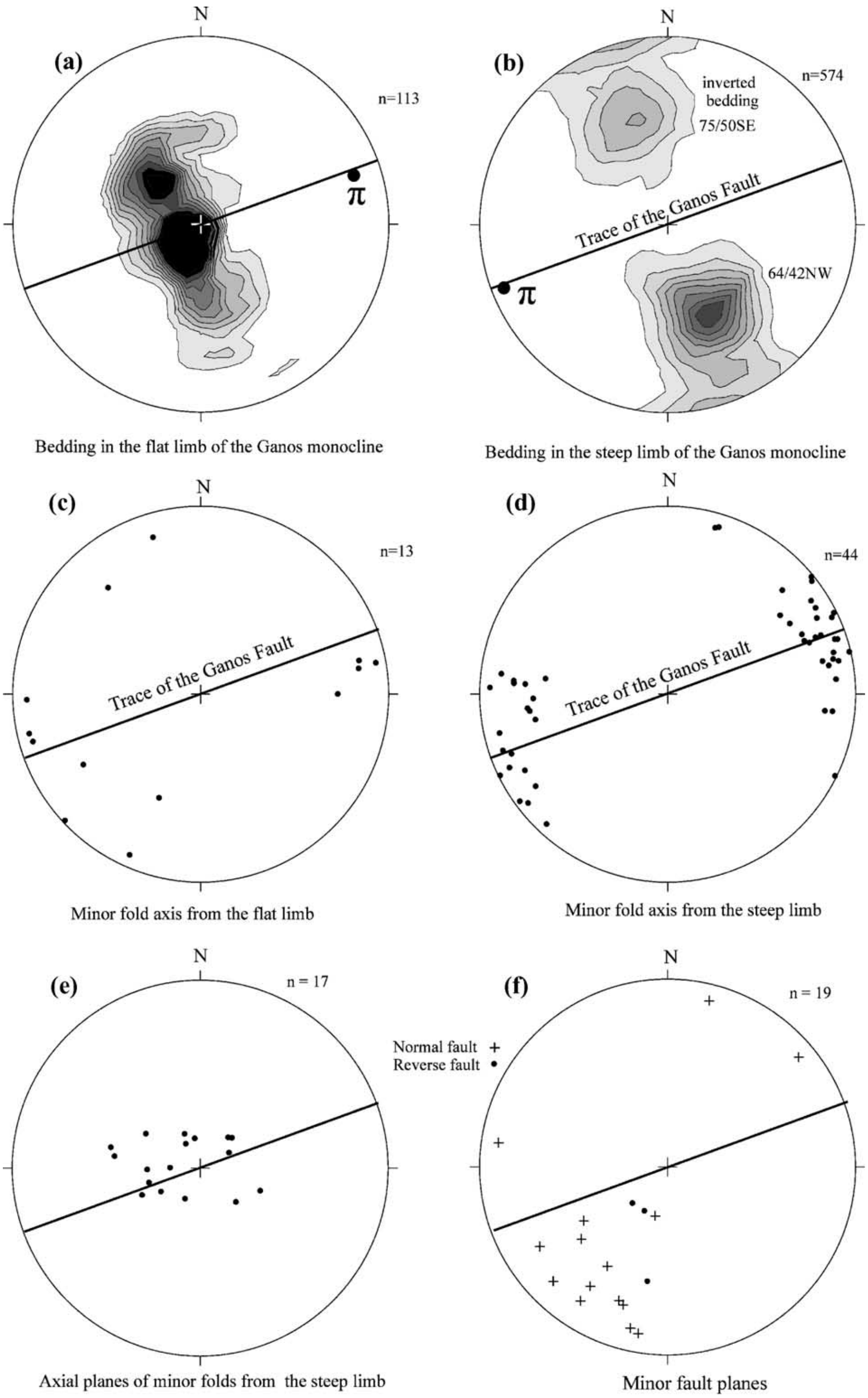
N
(a)
n=113
π
Bedding in the flat limb of the Ganos monocline
N
(b)
n=574
inverted bedding
75/50SE
Trace of the Ganos Fault
64/42NW
π
Bedding in the steep limb of the Ganos monocline
N
(c)
n=13
Trace of the Ganos Fault
Minor fold axis from the flat limb
N
(d)
n=44
Trace of the Ganos Fault
Minor fold axis from the steep limb
N
(e)
n = 17
Axial planes of minor folds from the steep limb
N
(f)
n = 19
Normal fault +
Reverse fault •
Minor fault planes

(Fig. 6). This observation suggests a transition about 10 km north of the North Anatolian Fault from pre-transform structures apparently unaffected by this fault to those controlled by it. We have mapped and studied in detail the well-exposed eastern part of the Ganos Mountain, where the transition from the flat-lying northern hinterland, with apparent pre-transform structures, to Ganos Mountain is exceptionally clear. The aim was to determine whether the structures in Ganos Mountain have formed through the activity of the North Anatolian Fault, and if so what are their implications for its geometry and kinematic evolution.

In the Barbaros–Yeniköy region, studied in detail, the bedding is subhorizontal in the flat limb of the monocline north of Naip Stream (Fig. 7). This bedding strikes generally northwest at high angles to the front of Ganos Mountain and the Ganos Fault. However, as the monoclinal axis is approached the bedding rotates to northeasterly strike and is deformed into upright gentle folds with subvertical axial planes and northeast-trending axes. This is well illustrated by the lumachelle horizon, which marks the base of the Osmancık Formation (Fig. 7). North of the Naip Stream, this horizon strikes north–south and forms part of the southeast limb of the large anticline described above (cf. Fig. 6). Traced south of the Naip Stream this bed is refolded into upright folds, which become increasingly tighter towards the monoclinal axis (Fig. 7). This refolding of older folds is regarded as an effect of the North Anatolian Fault. The bedding in the flat belt of the monocline forms a girdle around a fold axis with an average ENE plunge of 12° and average trend of N72°E, parallel to the trace of the Ganos Fault (Fig. 8a). The minor fold axes in the flat zone typically trend northeast but are more dispersed compared with those from the steep zone, possibly as a result of interference by earlier folds (Fig. 8c).

The transition from the flat limb to the steep limb of this monocline is abrupt and closely coincides with the change in slope angles (Fig. 3b). In the past a fault has been placed north of the Ganos Mountain to explain these abrupt changes in topography and structural style (e.g., Şaroğlu et al., 1992; Şentürk et al., 1998; Yaltırak and Alpar, 2002). However, detailed sections that are well exposed in several stream channels crossing this hypothetical fault did not reveal any such structure. Furthermore, there is no significant stratigraphic omission or repetition along the boundary between the flat and steep zones, which would have been a characteristic of a major normal or reverse fault.

The steep limb of this monocline lies mostly in the turbidites of the Keşan Formation, where a range of sedimentary structures in the sandstones, including flute casts, groove and striation casts, load casts, slumps, graded bedding and cross-bedding, provide unambiguous way-up criteria. Sandstones in the transition zone between the Keşan and Mezardere formations contain abundant ripple marks, which provide further way-up criteria in these units. The sedimentary structures in the steep limb of the monocline indicate that the beds dipping south are invariably inverted, and those dipping north are upright. The overturning, which characterizes about a third of the bedding, is local on the scale of a few metres to several hundred metres, and occurs on the limbs of recumbent folds with subhorizontal axial surfaces (Fig. 9). The average bedding in the steep limb strikes northeast (~70°) parallel to the trends of the Ganos Fault and of the mountain range. The normal and inverted beds form two distinct groups in Fig. 8b, with the average dip 42° towards N26°W for the normal bedding and 50° towards S15°E for the inverted bedding, giving an average regional fold axis with a plunge of 4° towards S69°W, parallel to the trace of the Ganos Fault. The average dip based on more than 550 measurements is 53°. Forty-four mesoscopic fold axes measured in the field show a variation in trend from N50°E to S84°E with a mean trend of N70°E and a mean plunge of 10° to the ENE,

Fig. 8. Structural data from the northeastern part of Ganos Mountain, from the region in Fig. 7, shown as lower hemisphere, equal area projections. Thick line in all projections shows the N70°E strike of the Ganos Fault. Contour plots of poles to bedding in the flat (a) and steep limb (b) of the Ganos monocline. The contours are at 1% intervals, and π marks the regional fold axis. The average pole to this normal bedding plunges at 48° towards S26°E whereas the average pole to this inverted bedding plunges at 40° towards N15°W. The average dips are thus 42° towards N26°W for the normal bedding and 50° towards S15°E for the inverted bedding, as stated in the text. (c) Axes of the upright folds in the flat limb of the monocline. (d) Axes of the recumbent folds in the steep limb of the monocline. (e) Poles to axial planes of folds in the steep limb of the monocline. Note the predominance of poles plunging to the northwest, indicating a preponderance of axial planes dipping to the southeast. (f) Poles to minor fault planes.

Fig. 9. Photograph of typical recumbent folds in the Eocene turbidites in Ganos Mountain. The folds are characterized by subhorizontal axial surfaces and hinge lines. The hinge lines are parallel to the trace of the Ganos Fault. In the folds the south dipping limbs are invariably inverted. Note the boudinage in the fold hinge in (a) under the hammer, and the stronger brittle deformation in the inverted limb in (b).

similar to the "average" fold axis trend of N69°E and plunge of 4° to the WSW inferred from the bedding (Fig. 8d). The fold axial planes are dispersed around the horizontal with a predominance of southeast dips (Fig. 8e).

The folds have formed in the interbedded sandstone and shale beds, and have wavelengths and amplitudes ranging from metres to hundreds of metres (Fig. 9). These folds are generally parallel, with straight limbs and sharp angular hinges with the interlimb angles of 65° to 120°. The strongly lithified sandstone beds maintain their thickness through the fold, whereas the shale interbeds locally show minor thickening in the fold hinges. Locally, fractures in the outer arcs of the folded sandstone beds are filled by shale (Fig. 9a). These fractures are subparallel to the fold axes, suggesting that they have been produced through buckling rather than through extension parallel to the fold axes. Structures indicative of extension parallel to fold axes, produced during rotation and considered characteristic of strike-slip components of deformation (e.g., Harland, 1971; Jamison, 1991), were not observed. No cleavage is associated with the folds. Folds are arranged en echelon, so that even the largest fold trace cannot be followed by more than a kilometre (Fig. 7), and they usually die out laterally and vertically over short distances. The sandstone beds have been folded by flexural slip mechanism, whereas a combination of flexural slip and flow was involved in the folding of shale beds (e.g., Donath and Parker, 1964). The absence of extension parallel to fold axes indicates folding in a plane strain environment of NNW–SSE shortening during a single phase of progressive deformation. The flexural-slip mechanism and the general absence of axial-plane cleavage indicate that the deformation occurred under conditions of low temperature and pressure.

Folds formed in strike-slip shear zones have been thought to share some common features, such as fold axes oblique to the shear direction, extension parallel to the fold axes, and upright fold geometry (e.g., Sylvester, 1988; Jamison, 1991). The minor folds observed in Ganos Mountain do not show any of these features. As illustrated schematically in Fig. 10, we suggest that these folds were formed during the northward tilting, by ~50°, of the well-stratified sandstone–shale sequence, under the influence of a horizontal (NNW–SSE) shear couple (Fig. 10). They represent kink-type folds, which accommodate top to the northwest shortening on the steep limb of the monocline. Some of the larger recumbent folds show stronger cataclasis in their inverted limbs (Fig. 9b), supporting the role of shear in their formation. The general SSE dips of the fold axial planes (Fig. 8e) are consistent with the model.

Faults are uncommon in the eastern part of Ganos Mountain. They are mostly minor normal faults with throws from a few centimetres to several metres. They post-date the formation of the recumbent folds. These fault planes dip generally to the northeast (Fig. 8f), and the average normal fault orientation (strike S58°E, dip 65° to the NNE) subtends an angle of 52° with the trace of the Ganos Fault. Normal faults of similar orientation (strike S55°E, dip 69° to the NNE) are more common farther west in Ganos Mountain near the Ganos Fault (cf. Fig. 14 of Okay et al., 1999). They may be related to secondary extension in a dextral transpressive regime, and/or to the subsidence of the Ganos Mountain near the Ganos bend. Normal faults striking typically towards S31°E, nearly perpendicular to the Ganos Fault, have been described in the Miocene sandstones south of this fault (Hancock and Erkal, 1990) and in the Gelibolu

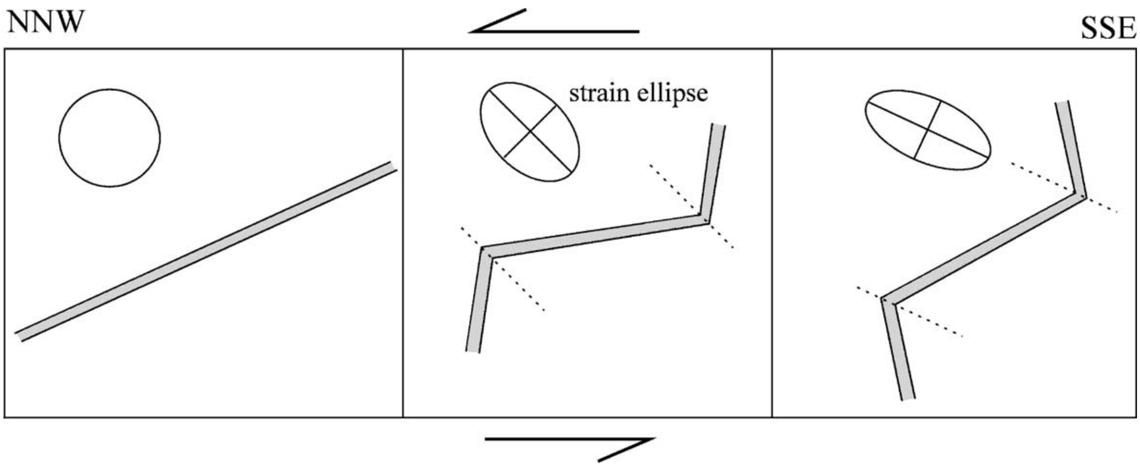

Fig. 10. Schematic model showing the formation of recumbent folds in Ganos Mountain. Each panel shows a part of a schematic NNW–SSE cross section through this region, viewed from the WSW, at different time-steps, with time and deformation increasing between panels from left to right. See text for discussion.

Peninsula (Tüysüz et al., 1998). Although the Ganos Fault is under transpression, reverse faults are rare in Ganos Mountain; the shortening is achieved largely by folding.

3.4. Origin of the Ganos monocline

The Ganos monocline is interpreted as a crustal ramp above the northward dipping North Anatolian Fault (Fig. 11b; Şengör, 1979). The argument that leads to this conclusion assumes that the structures seen in Ganos Mountain, including folding and the attitude of the bedding, reflect the finite strain imposed by the slip on the North Anatolian Fault. The parallel alignments of the trace of the Ganos Fault (N70°E), the strike of the bedding in Ganos Mountain (~N70°E), the trends of regional (N69°E) and minor (~N70°E) fold axes in Ganos Mountain, and the margins of this mountain itself indicate that these structures have formed as a result of shortening perpendicular to the Ganos Fault. Prior to the slip on the North Anatolian Fault, the bedding in the Ganos Mountain was most probably subhorizontal, as seen today in the flat limb of the Ganos monocline. We can use the geometry of this monocline to constrain the base of the ramp and the overall dip of the Ganos

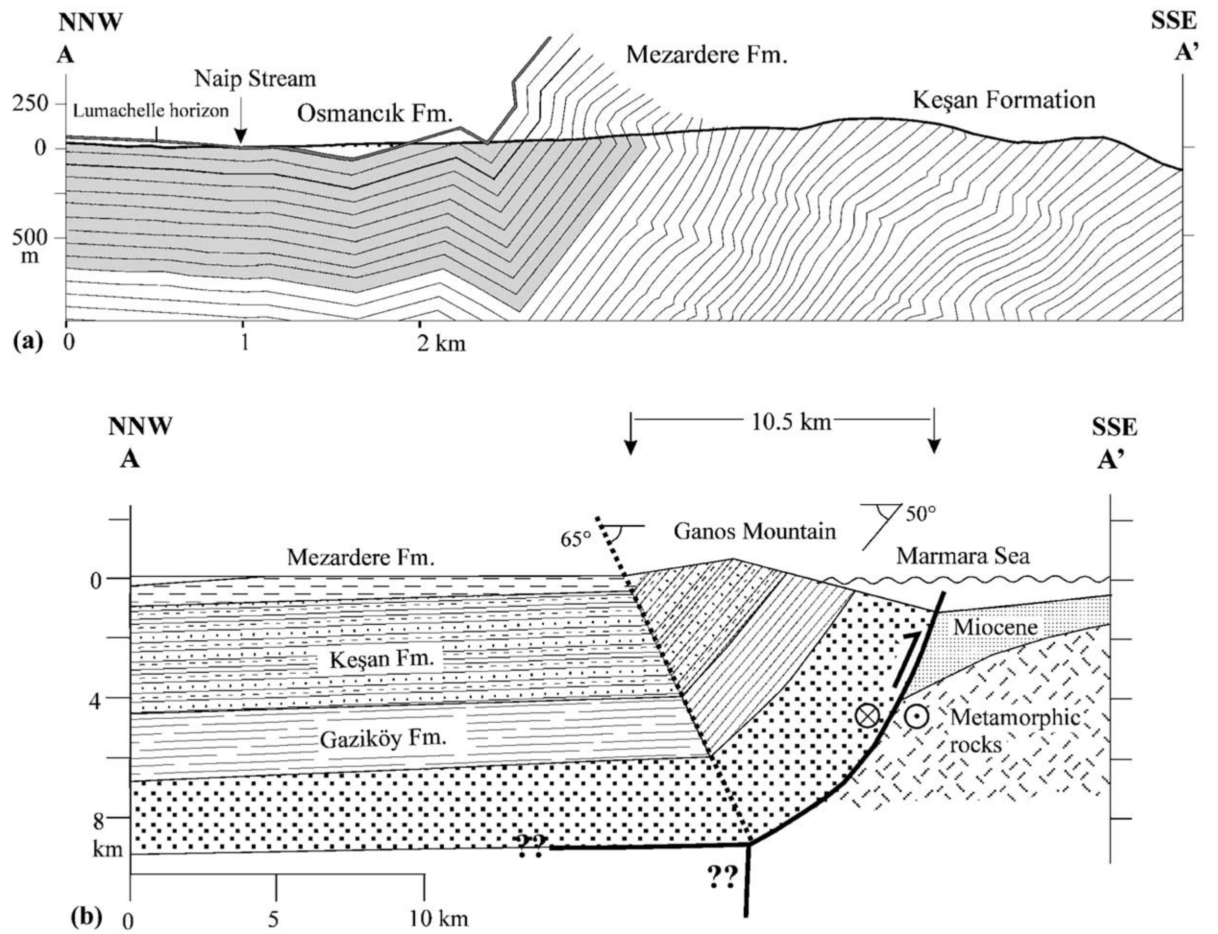

Fig. 11. (a) Geological cross-section across the eastern part of the Ganos Mountain. For the location of the section see Fig. 7. (b) Speculative, crustal scale geological cross section across the Ganos Mountain. The evidence is consistent with a planar dip of the ramp, rather than the listric geometry that is schematically shown. With such a planar geometry, the downdip length of the axial plane can be estimated using standard trigonometry as 2×10.5 km×cos 65° (or 10.5 km×sin 50°/sin 65°) and is ~8.9 km; the depth of its base is thus ~8.9 km×sin 65° or ~8.0 km. See Fig. 6 for the location of the section.

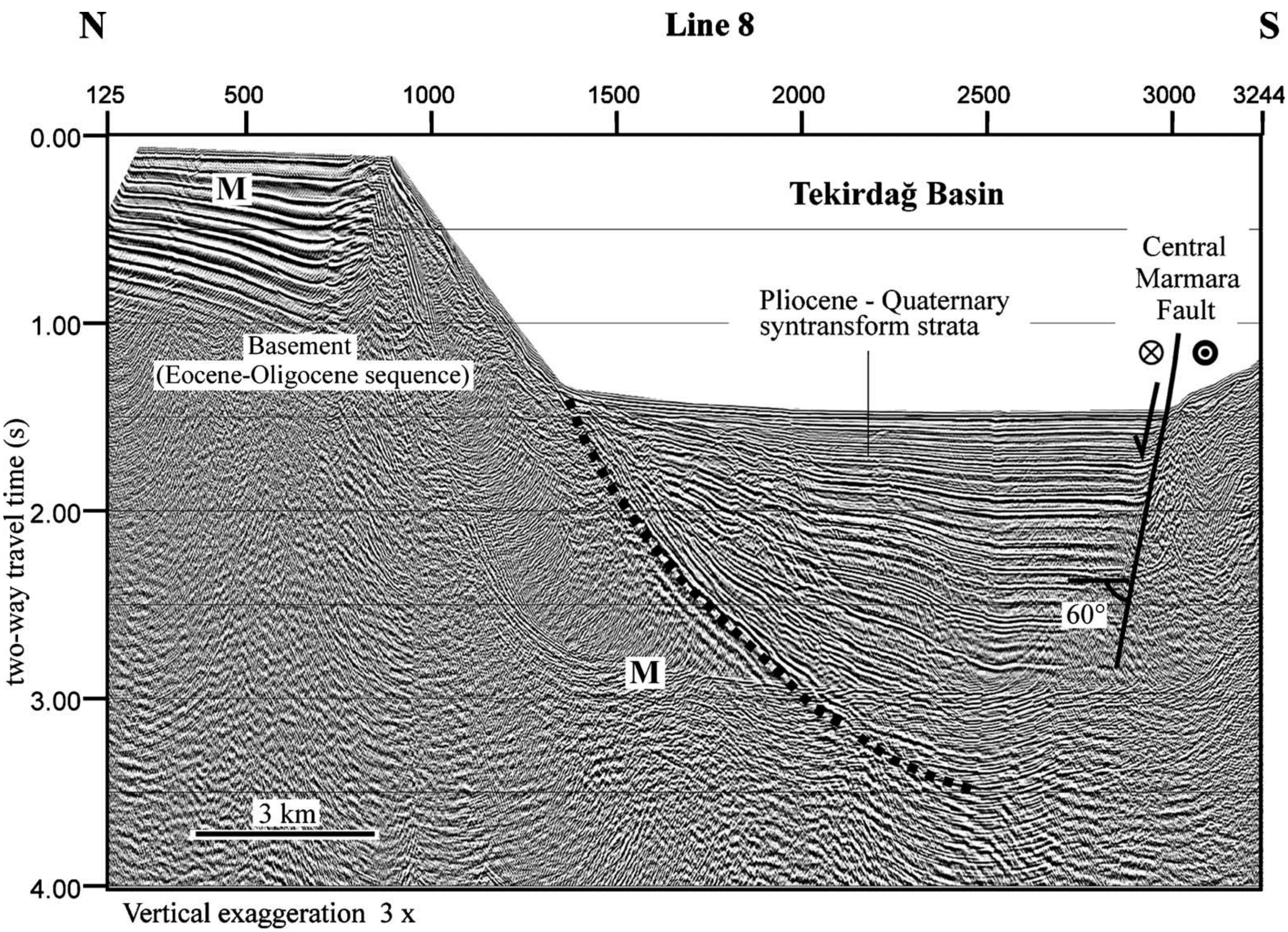

Fig. 12. Time-migrated seismic reflection section of line 8. The digits are common depth point (CDP) numbers. Multiple reflections are indicated by M. The vertical exaggeration shown is an average and approximate value for the syn-transform sediments. See Fig. 3a for the profile location. See Okay et al. (1999) for details regarding seismic data collection and processing.

Fault. We take the dip of the Ganos Fault to be subparallel to the bedding in Ganos Mountain, which typically dips at ~50°. This is a reasonable assumption as the Ganos Mountain is made up of well-indurated sandstone and shale forming a thick, rather homogeneous, competent sequence with a very strong planar anisotropy. The width of the steep limb of the monocline is ~10 km. The folding is assumed to be of parallel type, as observed in outcrop, so that the monoclinal axial plane dips south at 65°. These set of parameters indicate ~8 km depth of the base of the ramp (see calculation in Fig. 11 caption). The largest uncertainty in this calculation is caused by the dip of the Ganos Fault, which has been assumed parallel to the bedding in Ganos Mountain. However, increasing or decreasing this dip by 5° affects the calculated depth by less than 1 km, so that a ramp depth of 8 ± 1 km, and a dip of $50\pm5°$, is deduced for the Ganos Fault. Such a geometry indicates a minimum shortening of 3.6 km perpendicular to the Ganos Fault, calculated as $10\ \text{km}\times(1-\cos 50°)$, 50° being the estimated tilt of the beds that has accompanied this shortening and ~10 km being the estimated width of this zone of shortening. At the present rate of contraction (1.1 ± 0.4 mm/yr, estimated earlier) this could be achieved in 3.3 ± 1.0 My, providing a minimum age bound to this part of the North Anatolian Fault. The linear trace of the Ganos Fault indicates a steep dip near the Earth's surface. The 50° typical dip inferred for this fault between the Earth's surface and ~8 km depth thus implies a listric profile (as illustrated schematically in Fig. 11), consistent with the listric geometry of the North Anatolian Fault in the Tekirdağ Basin (Seeber et al., 2004). This interpretation of the Ganos Fault seems comparable with the listric thrusts described in the Transverse Ranges in California (Seeber and Sorlien, 2000).

4. Transtension: the Tekirdağ Basin, an active half-graben

Ganos Mountain is bounded in the east by the Tekirdağ Basin, a rhomb-shaped depression with a side-length of ~15 km and an area of ~220 km^2 (Figs. 2 and 3). The Tekirdağ Basin has a flat-lying floor at ~1100 m depth bordered in the north and south by steep submarine margins. The Central Marmara Fault constitutes the southern margin of the Tekirdağ Basin, and the basin floor rises gently south of this fault towards the southern shelf at −100 m. In the north the Tekirdağ Basin is bounded by the steep northern submarine slope with slope angles of 11° to 23°.

The Tekirdağ Basin has been recently studied by multi-channel seismic reflection, high-resolution bathymetric, sparker and deep-towed seismic reflection surveys (Okay et al., 1999; Le Pichon et al., 2001; Armijo et al., 2002; Parke et al., 2002; Seeber et al., 2004). These studies have shown that this basin is filled with Pliocene to Recent syntransform strata up to 2.5 km thick. A representative multi-channel seismic reflection section at a high angle to the Central Marmara Fault is shown in Fig. 12. The basin fill is strongly asymmetric, with the syn-tectonic growth strata thickening from essentially zero at the edge of the northern slope to 2.5 km at the Central Marmara Fault (Fig. 12). In the top few kilometres, as observed in the seismic sections, the Central Marmara Fault dips north at ~60°, with the dip angles increasing eastward (Okay et al., 1999). As argued in Seeber et al. (2004), the strongly asymmetric basin fill, and the gradual downward increase in the dip of the syntransform beds, implies a shallower dip of the fault plane, and hence a listric fault profile. This is consistent with our data from Ganos Mountain, as discussed above.

In the seismic reflection sections the Central Marmara Fault is well marked as a line bounding the undeformed syntransform strata (Fig. 12; see also Okay et al., 1999). In seismic section 2, located close to the Ganos bend, undeformed syntransform strata is overlain by the Miocene submarine slide deposits (Fig. 13). This implies that the North Anatolian Fault must pass south of the seismic section 2, and not north of it as shown in recent publications (e.g., Okay et al., 1999; Le Pichon et al., 2001; Armijo et al., 2002; Demirbağ et al., 2003). The non-recognition of the submarine slide deposits led Okay et al. (1999) to infer a southward rather than a northward dip for the Ganos Fault. The modified position of the North Anatolian Fault around the fault bend is in better agreement with the data from land and the shelf regions (cf. Seeber et al., 2004) and with the inferred subsidence of the Ganos Mountain.

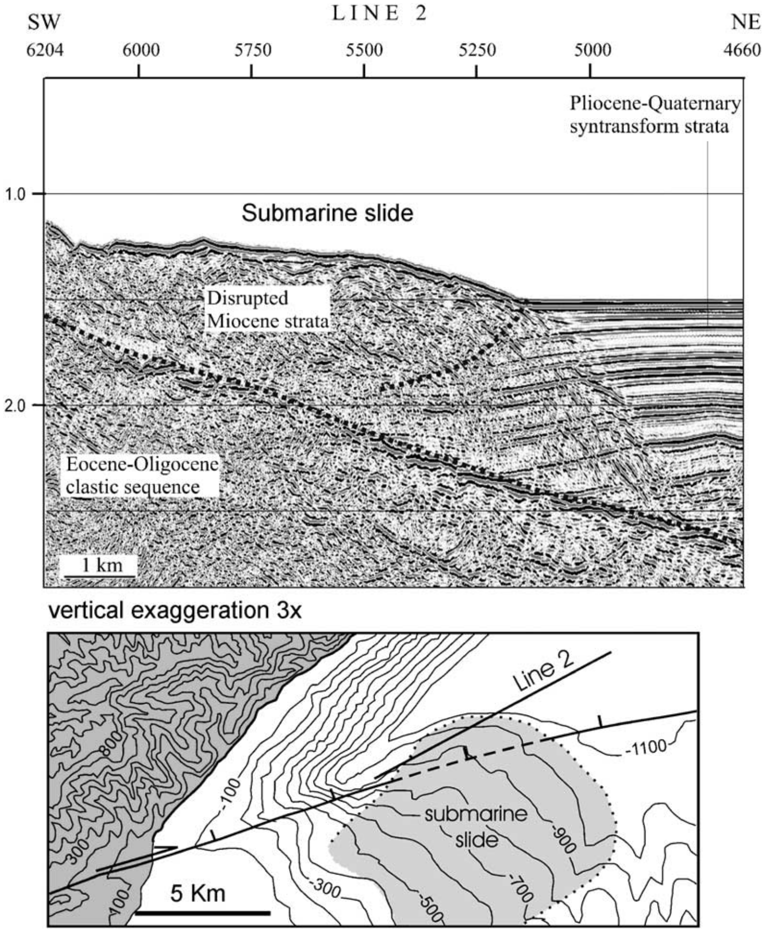

Fig. 13. Time-migrated seismic reflection section of the western part of line 2. The digits are common depth point (CDP) numbers. Multiple reflections are indicated by M. The vertical exaggeration shown is an average and approximate value for the syn-transform sediments. The map below shows the location of the seismic profile; see also Fig. 3a for the profile location (modified from Okay et al., 1999).

4.1. Origin of the northern submarine slope

As already noted, the Tekirdağ Basin is bounded in the north by a continuous steep submarine slope, which has slope angles of 11° to 23° (Fig. 3). The origin of this northern slope is controversial; there are suggestions that it may be caused by a southeast dipping low-angle normal fault (Wong et al., 1995; Ergün and Özel, 1995; Okay et al., 1999), or a northwest dipping thrust fault (Şengör et al., 1985; Le Pichon et al., 2001; Armijo et al., 2002; Demirbağ et al., 2003). A thrust fault with a significant displacement at the base of the northern slope can be ruled out as the seismic sections show no overthrusting of the syntransform sediments by the Eocene–Oligocene basement (Okay et al., 1999). A detachment fault subparallel to the northern slope is also unlikely, as the syntransform strata do not show any deformation that would be expected from gravity sliding.

We thus suggest that this northern submarine slope of the Tekirdağ Basin is a morphological relic of the former counterpart to the Ganos uplift from earlier in the evolution of the North Anatolian Fault, which was translated eastward from the transpressive to the transtensional fault segment. Fig. 14 is a scaled model showing the suggested evolution of the morphology around the Ganos fault bend. As the Ganos uplift is translated east of the bend, it undergoes southward

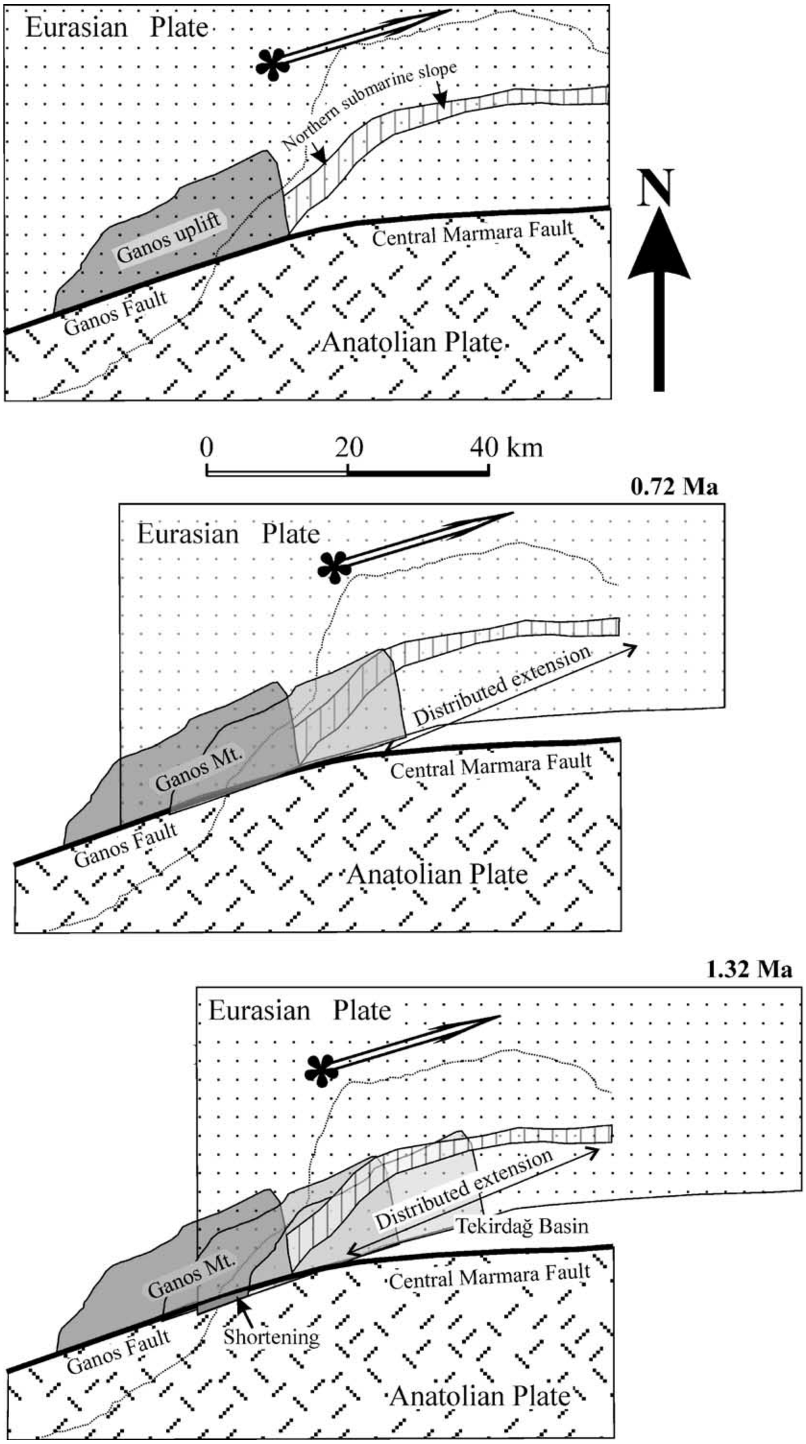

Fig. 14. Scaled model illustrating the origin of the northern submarine slope of the Tekirdağ Basin by subsidence and eastward translation of the Ganos Mountain. Note that the length of the northern submarine slope indicates that the Ganos uplift has existed for at least since the last 2 million years.

tilting, leading to subsidence along the Central Marmara Fault, and most of the former mountain is buried under the younger syn-transform sediments. Seismic section 2 shows the strong onlap of these syntransform strata onto the southern flank of the Ganos Mountain (Fig. 13). Only the northern part of this former mountain now "sticks out" of the sea bottom, forming the northern submarine slope of the Tekirdağ Basin. The morphology of the Tekirdağ Basin indicates that the Ganos uplift has been translated eastward for at least 40 km (Figs. 2 and 3). Therefore, the Ganos bend has been locked in position and has been in existence for at least the last 2 million years (~40 km/~20 mm/yr), in rough agreement with the time frame deduced from the shortening in the Ganos Mountain.

The North Anatolian Fault east of the Ganos bend could theoretically follow any line between the northern and southern margins of the Tekirdağ Basin (Fig. 14). The fact that it follows the southern, rather than the northern margin of the Tekirdağ Basin indicates that the Ganos bend is fixed to the Anatolian Plate. This is in agreement with the stronger transform-related contractional and extensional deformation observed north of the Ganos bend, as compared to that south of the bend. The well-developed shelf south of the Ganos Fault, compared with the lack of it north of the Fault, also indicates that the Anatolian Block south of the Ganos bend acts as a rigid indenter (Seeber et al., 2004). This is probably related to the more competent upper crustal structure of the Anatolian Block south of the Ganos bend, which is composed of metamorphic and granitic rocks with a thin cover of Miocene sediments.

5. Discussion and conclusions

We have used GPS measurements, morphology and structural geology to understand deformation at the 17° Ganos bend on the North Anatolian Fault in the western Marmara region. These three data sets reflect deformation integrated over different time scales. The GPS measurements show a small amount of transpression (3°) along the Ganos Fault. The structures in the rocks, which reflect the finite strain imposed by the North Anatolian Fault during the Pliocene–Quaternary, indicate shortening of at least 3.6 km perpendicular to this fault. We suggest that this shortening is achieved by rotation of bedding from subhorizontal to steep north dips (50°) and by minor folding. This tilting of bedding occurs by oblique slip (reverse and strike-slip) on the northward-dipping Ganos fault plane, producing a crustal-scale ramp. Calculations suggest a depth of 8 ± 1 km for the base of this ramp, and a northward dip of $50\pm5°$ for the North Anatolian Fault plane. The ramp either soles at the base of the seismogenic crust or passes into a steeper fault at depth (cf. Seeber et al., 2004). Although considerably shallower than 15 km usually assumed for the Marmara region, this 8-km-depth limit is similar to that deduced by Meade et al. (2002) for the base of the seismogenic layer using the GPS data. The Ganos Fault zone forms a seismic gap with very few earthquakes in the instrumental period (e.g. Gurbuz et al., 2000). The only fault plane solution on the Ganos Fault, that of the 27 April 1985 Mürefte earthquake (M=4.4) located in the Ganos Mountain, gives a reverse fault mechanism with a NE striking fault plane (Kalafat, 1995), consistent with our data. Furthermore, an inclined fault plane, and oblique slip, is not peculiar to the Ganos Fault segment; they are also inferred for the 12 November 1999 M_w 7.2 Düzce earthquake on the North Anatolian Fault. Teleseismic waveform inversions, GPS and InSAR data indicate that the rupture in this Düzce earthquake occurred on a 54° north-dipping fault, striking obliquely to the typical trend of the North Anatolian Fault (Bürgmann et al., 2002).

The Tekirdağ Basin is a large half-graben forming along the transtensional Central Marmara Fault segment of the North Anatolian Fault. Ganos Mountain is being translated east of the Ganos fault bend while undergoing subsidence along the north-dipping Central Marmara Fault, for which a listric geometry is deduced, and thus being covered by syn-transform sediments of the Tekirdağ Basin. The northward dip of the main fault plane is maintained on both sides of this bend, but the dip-slip vectors on both sides of the bend are in opposite directions (Seeber et al., 2004). The minimum of ~3.5 km of shortening estimated at Ganos Mountain, and the minimum 40 km eastward translation of the Ganos uplift, indicates that the present geometry of the North Anatolian Fault in the western Marmara Sea has been in existence for at least the last 2 million years.

The main factor that controls the degree of strain partitioning in strike-slip fault zones is thought to be the angle of obliquity, α, between the plate margin and the plate-motion vector, with the low angles promoting strain partitioning (e.g., Richard and Cobbold, 1990; Teyssier et al., 1995). However, although the obliquity is low at the eastern end of the Ganos Fault (α=3°±1°), this fault shows no strain partitioning. This could be due to inherited fault geometry from the Central Marmara Fault, where the obliquity is higher (α=14°±2°). Westward along strike, the dip of the Ganos Fault plane increases and becomes subvertical. In this region the shortening perpendicular to the fault is accommodated by oblique folds and thrusts in the strike-slip fault zone (Fig. 2).

Based on satellite imagery, Armijo et al. (1999) suggested that Ganos Mountain represents the northern half of a truncated anticline, whose southern half has been displaced to the Gelibolu peninsula, and used this displacement to estimate the cumulative offset on the Ganos Fault. However, as described above, the geology of Ganos Mountain does not support an interpretation as an anticline; it is instead a monocline. Furthermore, the axes of the folds formed in a shear zone usually make an angle of 10° to 35° with the shear direction (e.g., Sylvester, 1988; Jamison, 1991). In Ganos Mountain the major monoclinal axis and the axes of the minor folds are parallel to the North Anatolian Fault, suggesting that the folds did not form before the initiation of the North Anatolian Fault. An additional argument against equating the Gelibolu peninsula with the Ganos Mountain is the differing Eocene–Oligocene lithostratigraphy exhibited in the two areas (cf. Yaltırak et al., 2000). The Ganos fault bend has remained localised on the Anatolian side of the North Anatolian Fault (Seeber et al., 2004), possibly because its crust is stronger, and the associated deformation has thus been concentrated on its Eurasian side, in Ganos Mountain. This mountain thus need not have any counterpart on the Anatolian side of this fault.

This study demonstrates the brief lifetime of restraining bend mountain ranges, which pop up quickly and then subside soon after, as they pass around the bend. In the geological record this may be marked by a major unconformity, which youngs towards the fold bend. The unconformity between the syn-transform strata of the Tekirdağ Basin, and the underlying Eocene–Oligocene sequence, provides such an example. Sequences beneath the unconformity will be characterized by contractional structures overprinted by tensional structures, whereas those above the unconformity by only tensional structures, both being transform related.

Acknowledgements

We thank the Istanbul Technical University Research Fund (project no. 2002) and Turkish Academy of Sciences for supporting the fieldwork. We are grateful to Korhan Erturaç for assisting in digitising the bathymetric maps, Claude Rangin for help with the bathymetric data, Boris Natalin and Nilgün Okay for helpful discussions, Dickson Cunningham for a constructive review, and Rob Westaway for editorial assistance.

References

Aksoy, Z., 1987. Depositional environment of the sequences in the Barbaros–Keşan–Kadköy–Gaziköy region (southern Thrace). Proceedings of the 7th Petroleum Congress of Turkey. Turkish Association of Petroleum Geologists, Ankara, pp. 292–311 (in Turkish).

Allen, C.R., 1975. Geological criteria for evaluating seismicity. Geol. Soc. Amer. Bull. 86, 1041–1057.

Ambraseys, N., 2002. The seismic activity of the Marmara Sea region over the last 2000 years. Bull. Seismol. Soc. Am. 92, 1–18.

Ambraseys, N.N., Finkel, C.F., 1987. The Saros–Marmara earthquake of 9 August 1912. Earthquake Eng. Struc. Dyn. 15, 189–211.

Armijo, R., Meyer, B., Hubert, A., Barka, A., 1999. Westward propagation of the North Anatolian fault into the northern Aegean: timing and kinematics. Geology 27, 267–270.

Armijo, R., Meyer, B., Navarro, S., King, G., Barka, A., 2002. Asymmetric slip partitioning in the Sea of Marmara pull-apart: a clue to propagation processes of the North Anatolian Fault? Terra Nova 14, 80–86.

Barka, A.A., 1992. The North Anatolian fault Zone. Ann. Tecton. 6, 164–195.

Bürgmann, R., Ayhan, M.E., Fielding, E.J., Wright, T.J., McClusky, S., Aktug, B., Demir, C., Lenk, O., Türkezer, A., 2002. Deformation during the 12 November 1999 Düzce, Turkey earthquake, from GPS and InSAR data. Bull. Seismol. Soc. Am. 92, 161–171.

Demirbağ, E., Rangin, C., Le Pichon, X., Şengör, A.M.C., 2003. Investigation of the tectonics of the Main Marmara Fault by means of deep-towed seismic data. Tectonophysics 361, 1–19.

Donath, F.A., Parker, R.B., 1964. Folds and folding. Geol. Soc. Amer. Bull. 75, 45–62.

Ergün, M., Özel, E., 1995. Structural relationships between the Sea of Marmara Basin and the North Anatolian Fault Zone. Terra Nova 7, 278–288.

Gazioğlu, C., Gökaşan, E., Algan, A., Yücel, Z., Tok, B., Doğan, E., 2002. Morphological features of the Marmara Sea from multi-beam data. Mar. Geol. 190, 397–420.

Görür, N., Okay, A.I., 1996. A fore-arc origin for the Thrace Basin, NW Turkey. Geol. Rundsch. 85, 662–668.

Gurbuz, C., Aktar, M., Eyidogan, H., Cisternas, A., Haessler, H., Barka, A., Ergin, M., Turkelli, N., Polat, O., Ucer, S.B., Kuleli, S., Baris, S., Kaypak, B., Bekler, T., Zor, E., Bicmen, F., Yoruk, A., 2000. The seismotectonics of the Marmara region (Turkey): results from a microseismic experiment. Tectonophysics 316, 1–17.

Hancock, P.L., Erkal, T., 1990. Enigmatic normal faults within the European sector of the North Anatolian transform fault zone. Ann. Tecton. 4, 171–181.

Harland, W.B., 1971. Tectonic transpression in Caledonian Spitsbergen. Geol. Mag. 108, 27–42.

Hubert-Ferrari, A., Armijo, R., King, G., Meyer, B., Barka, A., 2002. Morphology, displacement, and slip rates along the North Anatolian Fault, Turkey. J. Geophys. Res. 107 (B10) art. no. 2235, 10.1029/2001 JB000393.

İmren, C., Le Pichon, X., Rangin, C., Demirbağ, E., Ecevitoğlu, B., Görür, N., 2001. The North Anatolian Fault within the Sea of Marmara: a new interpretation based on multi-channel seismic and multi-beam bathymetry data. Earth Planet. Sci. Lett. 186, 159–173.

Jamison, W.R., 1991. Kinematics of compressional fold development in convergent wrench terranes. Tectonophysics 190, 209–232.

Kahle, H.G., Cocard, M., Peter, Y., Geiger, A., Reilinger, R., Barka, A., Veis, G., 2000. GPS-derived strain rate field within the boundary zones of the Eurasian, African and Arabian Plates. J. Geophys. Res. 105, 23353–23400.

Kalafat, D., 1995. Study of the tectonic structures in Anatolia based on fault mechanism solutions. PhD thesis. University of Istanbul, 217 pp. (in Turkish).

Keller, E.A., Gurrola, L., Tierney, T.E., 1999. Geomorphic criteria to determine the direction of lateral propagation of reverse faulting and folding. Geology 27, 515–518.

Kopp, K.O., Pavoni, N., Schindler, C., 1969. Geologie Thrakiens IV: Das Ergene Becken. Geol. Jahrb., Beih. 76, 1–136.

Lebküchner, R.F., 1974. Beitrag zur Kenntnis des Geologie des Oligozäns von MittelThrakien (Türkei). Bull. Miner. Res. Explor. Inst. Turk. 83, 1–30.

Le Pichon, X., Şengör, A.M.C., Demirbağ, E., Rangin, C., İmren, C., Armijo, R., Görür, N., Çağatay, N., Mercier de Lepinay, B., Meyer, B., Saatçiler, R., Tok, B., 2001. The active Main Marmara Fault. Earth Planet. Sci. Lett. 192, 595–616.

McClusky, S., 2000. Global Positioning System constraints on plate kinematics and dynamics in the eastern Mediterranean and Caucasus. J. Geophys. Res. 105, 5695–5719.

Meade, B.J., Hager, B.H., McClusky, S.C., Reilinger, R.E., Ergintav, S., Onur, L., Barka, A., Özener, H., 2002. Estimates of seismic potential in the Marmara Sea region from block models of secular deformation constrained by Global Positioning System measurements. Bull. Seismol. Soc. Am. 92, 208–215.

Okay, N., Okay, A.I., 2002. Tectonically induced Quaternary drainage diversion in northeastern Aegean. J. Geol. Soc. (Lond.) 159, 393–400.

Okay, A.I., Demirbağ, E., Kurt, H., Okay, N., Kuşçu, İ., 1999. An active, deep marine strike-slip basin along the North Anatolian fault in Turkey. Tectonics 18, 129–148.

Okay, A.I., Kaşlılar-Özcan, A., İmren, C., Boztepe-Güney, A., Demirbağ, E., Kuşçu, Ý., 2000. Active faults and evolving strike slip basins in the Marmara Sea, northwest Turkey: a multi-channel seismic reflection study. Tectonophysics 321, 189–218.

Parke, J.R., White, R.S., McKenzie, D., Minshul, T.A., Bull, J.M., Kuşçu, I., Görür, N., Şengör, C., 2002. Interaction between faulting and sedimentation in the Sea of Marmara, western Turkey. J. Geophys. Res. 107 (B11) art no. 2286, doi: 10.1029/2001 JB000450.

Polonia, A., Cormier, M.H., Çağatay, N., Bortoluzzi, G., Bonatti, E., Gasperini, L., Seeber, L., Görür, N., McHugh, C., Ryan, W.B., Emre, Ö., Okay, N., Ligi, M., Tok, B., Blasi, A., Busetti, M., Eriş, K., Fabretti, P., Fielding, E.J., İmren, C., Kurt, H., Magagnoli, A., Marozzi, G., Özer, N., Penitenti, D., Serpi, G., Sarıkavak, K., 2002. Exploring submarine earthquake geology in the Marmara Sea. EOS Transactions AGU 83 (21), 229 and 235–236.

Rangin, C., Demirbag, E., Imren, C., Crusson, A., Normand, A., Le Drezen, E., Le Bot, A., 2001. Marine Atlas of the Sea of Marmara (Turkey). IFREMER, Paris.

Richard, P., Cobbold, P., 1990. Experimental insights into partitioning of fault motions in continental convergent wrench zones. Ann. Tecton. 4, 35–44.

Rockwell, T., Barka, A., Dawson, T., Akyüz, S., Thorup, K., 2001. Paleoseismology of the Gaziköy–Saros segment of the North Anatolian fault, northwestern Turkey: comparison of the historical and paleoseismic records, implications of regional seismic hazard, and models of earthquake recurrence. J. Seismol. 5, 433–448.

Sakınç, M., Yaltırak, C., Oktay, F.Y., 1999. Palaeogeographical evolution of the Thrace Neogene basin and the Tethys-Paratethys relations at northwestern Turkey (Thrace). Palaeogeogr. Palaeoclimatol. Palaeoecol. 153, 17–40.

Şaroğlu, F., Emre, Ö., Kuşçu, İ., 1992. Active fault map of Turkey. 2 sheets, scale 1: 2,000,000. General Directorate of Mineral Research and Exploration, Ankara.

Seeber, L., Sorlien, C., 2000. Listric thrusts in the western Transverse Ranges, California. Geol. Soc. Amer. Bull. 112, 1067–1079.

Seeber, L., Emre, O., Cormier, M., Sorlien, C., McHugh, C., Polonia, A., 2004. Uplift and subsidence from oblique slip: the Ganos–Marmara bend of the North Anatolian Transform, western Turkey. Tectonophysics 391, 239–258, this issue.

Şengör, A.M.C., 1979. The North Anatolian transform fault: its age, offset and tectonic significance. J. Geol. Soc. (Lond.) 136, 269–282.

Şengör, A.M.C., Görür, N., Şaroğlu, F., 1997. Strike-slip faulting and related basin formation in zones of tectonic escape: Turkey as a case study. In: Biddle, K.D., Christie-Blick, N. (Eds.), Strike-Slip Deformation, Basin Formation, and Sedimentation, Spec. Publ. - Soc. Econ. Paleontol. Mineral. vol. 17. 1985 pp. 227–264.

Şentürk, K., Sümengen, M., Terlemez, İ., Karaköse, C., 1998. Bandırma D-4 sheet and 10 page explanatory text, 1:100,000 scale geological map series. General Directorate of Mineral Research and Exploration, Ankara.

SHOD, 1983. Bathymetric chart of the Marmara Sea between Büyükçekmece and Hoşköy, scale 1:100 000. Map no. 291, Turkish Navy, Department of Navigation, Hydrography and Oceanography [Seyir, Hidrografi ve Oşinografi Dairesi Başkanlığı], Istanbul.

SHOD, 1988, Bathymetric chart of the Marmara Sea between Hoşköy and Gelibolu, scale 1:75 000. Map no. 295, Turkish Navy, Department of Navigation, Hydrography and Oceanography [Seyir, Hidrografi ve Oşinografi Dairesi Başkanlığı], Istanbul.

Straub, C., 1996. Recent crustal deformation and strain accumulation in the Marmara Sea region, N.W. Anatolia, inferred from GPS measurements. PhD thesis, Swiss Federal Institute of Technology, Zürich. ETH dissertation no. 11614, 123 pp.

Straub, C., Kahle, H.-G., Schindler, C., 1997. GPS and geologic estimates of the tectonic activity in the Marmara region, NW Anatolia. J. Geophys. Res. 102, 27587–27601.

Sylvester, A.G., 1988. Strike-slip faults. Geol. Soc. Amer. Bull. 100, 1666–1703.

Teyssier, C., Tikoff, B., Markley, M., 1995. Oblique plate motion and continental tectonics. Geology 23, 447–450.

Turgut, S., Türkaslan, M., Perinçek, D., 1998. Evolution of the Thrace sedimentary basin and its hydrocarbon prospectivity. In: Spencer, A.M. (Ed.), Generation, Accumulation, and Production of Europe's Hydrocarbons, Spec. Publ. Eur. Ass. Petrol. Geosci. vol. 1. 1991 pp. 415–437.

Tüysüz, O., Barka, A., Yiğitbaş, E., 1998. Geology of the Saros Graben: its implications on the evolution of the North Anatolian Fault in the Ganos–Saros region, NW Turkey. Tectonophysics 293, 105–126.

Westaway, R., 1994. Present-day kinematics of the Middle East and eastern Mediterranean. J. Geophys. Res. 99, 12071–12090.

Westaway, R., 1995. Deformation around stepovers in strike-slip fault zones. J. Struct. Geol. 17, 831–846.

Westaway, R., 2003. Kinematics of the Middle East and Eastern Mediterranean updated. Turk. J. Eart. Sci. 12, 5–46.

Westaway, R., 2004. Kinematic consistency between the Dead Sea Fault Zone and the Neogene and Quaternary left-lateral faulting in SE Turkey. Tectonophysics, 391, 203–237 this issue.

Wong, H.K., Lüdmann, T., Ulug, A., Görür, N., 1995. The Sea of Marmara: a plate boundary sea in an escape tectonic regime. Tectonophysics 244, 231–250.

Yaltırak, C., 1995. Sedimentary and tectonics features of the region between Gaziköy and Mürefte (Tekirdağ). Türkiye Petrol Jeologları Derneği Bülteni 6, 93–112. (in Turkish).

Yaltırak, C., 2002. Tectonic evolution of the Marmara Sea and its surroundings. Mar. Geol. 190, 493–529.

Yaltırak, C., Alpar, B., 2002. Kinematics and evolution of the northern branch of the North Anatolian Fault (Ganos Fault) between the Sea of Marmara and the Gulf of Saros. Mar. Geol. 190, 352–366.

Yaltırak, C., Sakınç, M., Oktay, F.Y., 2000. Westward propagation of the North Anatolian fault into the northern Aegean: timing and kinematics, Comment. Geology 28, 187–188.